J Neurophysiol 94: 2738–2747, 2005.
First published July 6, 2005; 10.1152/jn.00362.2005.

Affects of Aging on Receptive Fields in Rat Primary Auditory Cortex Layer V Neurons

Jeremy G. Turner,[1,2] Larry F. Hughes,[2] and Donald M. Caspary[1,2]
[1]*Departments of Pharmacology and* [2]*Surgery, Southern Illinois University School of Medicine, Springfield, Illinois*

Submitted 8 April 2005; accepted in final form 27 June 2005

Turner, Jeremy G., Larry F. Hughes, and Donald M. Caspary. Affects of aging on receptive fields in rat primary auditory cortex layer V neurons. *J Neurophysiol* 94: 2738–2747, 2005. First published July 6, 2005; 10.1152/jn.00362.2005. Advanced age is commonly associated with progressive cochlear pathology and central auditory deficits, collectively known as presbycusis. The present study examined central correlates of presbycusis by measuring response properties of primary auditory cortex (AI) layer V neurons in the Fischer Brown Norway rat model. Layer V neurons represent the major output of AI to other cortical and subcortical regions (primarily the inferior colliculus). In vivo single-unit extracellular recordings were obtained from 114 neurons in aged animals (29–33 mo) and compared with 105 layer V neurons in young-adult rats (4–6 mo). Three consecutive repetitions of a pure-tone receptive field map were run for each neuron. Age was associated with fewer neurons exhibiting classic V/U-shaped receptive fields and a greater percentage of neurons with more Complex receptive fields. Receptive fields from neurons in aged rats were also less reliable on successive repetitions of the same stimulus set. Aging was also associated with less firing during the stimulus in V/U-shaped receptive field neurons and more firing during the stimulus in Complex neurons, which were generally associated with inhibited firing in young controls. Finally, neurons in aged rats with Complex receptive fields were more easily driven by current pulses delivered to the soma. Collectively, these findings provide support for the notion that age is associated with diminished signal-to-noise coding by AI layer V neurons and are consistent with other research suggesting that GABAergic neurotransmission in AI may be compromised by aging.

INTRODUCTION

Age-related hearing loss, *presbycusis*, affects approximately one third of all adults between the ages of 65 and 74 and one half over the age of 74, making it one of the most common ailments of the elderly (Corso 1982). Presbycusis is associated with both peripheral and central processing deficits that combine to make it difficult for the elderly to process speech and other acoustic signals in noisy or complex environments (Bergman et al. 1976; Divenyi and Haupt 1997a,b; Willott 1991). Although presbycusis has been associated with a variety of anatomical, biochemical, and electrophysiological changes in subcortical auditory structures (for reviews, see Seidman et al. 2002; Willott 1991), relatively little work has been done to outline the age-related electrophysiological changes in the primary auditory cortex (AI).

Aging in mice with high-frequency hearing loss has been associated with tonotopic reorganization of AI so that still intact lower and middle frequencies become overrepresented (Willott et al. 1993). In rats, aging was associated with deterioration of temporal processing speed in AI neurons, which they did not find in lower structures such as the inferior colliculus and auditory thalamus (Lee et al. 2002; Mendelson and Lui 2004; Mendelson and Ricketts 2001). Evidence also suggests that in humans aging is associated with a deficit in processing sound duration at auditory cortex, measured as an abnormal sound duration growth function of the P2 wave (Ostroff et al. 2003). These electrophysiological studies suggest that aging is associated with altered spectral and temporal properties of the auditory cortex, which might play a role in the numerous speech/auditory processing difficulties observed in the aged population.

The present study begins to outline the age-related electrophysiological changes in AI by focusing on receptive field characteristics, such as shape and variability, of single layer V neurons. A recent in vivo recording study demonstrated that in young-adult, normal hearing rats, AI layer V contained two major groups of receptive fields that together constitute nearly 80% of all neurons recorded (Turner et al. 2005). One of these groups consisted mostly of monotonic V/U-shaped receptive field maps (32%), which were reliable across repetitions and were easily depolarized with current pulses delivered to the soma. The second group consisted primarily of poorly defined receptive fields, which were more variable on repetition. These receptive fields were termed *Complex* and were difficult to depolarize either with acoustic or current stimulation, presumably because of greater GABAergic inhibitory influence (Hefti and Smith 2000, 2003). The focus of the present study was to determine the age-related changes in receptive fields of AI layer V cells. Layer V was chosen because of its role in integrating intracortical information across many cortical layers and projecting that information to other intra- and extracortical structures (Aitkin 1981; Doucet 2002; Games and Winer 1988; Herbert et al. 1991; Schofield and Coomes 2005) and because of previous anatomical work suggesting age-related deterioration of AI layer V cells (Vaughan 1977; Vaughan and Peters 1974; Vaughan and Vincent 1979). As the major output of auditory cortex to other auditory and nonauditory structures, age-related changes in the functional characteristics of this AI layer (vis-à-vis anatomical and neurochemical changes with age) might aid our understanding of some of the central processing deficits observed in the elderly.

Address for reprint requests and other correspondence: J. G. Turner, Departments of Pharmacology and Surgery–Otolaryngology, Southern Illinois University School of Medicine, Springfield, IL 62794-9629 (E-mail: jturner@siumed.edu).

The costs of publication of this article were defrayed in part by the payment of page charges. The article must therefore be hereby marked "*advertisement*" in accordance with 18 U.S.C. Section 1734 solely to indicate this fact.

METHODS

Subjects

Thirteen aged (29–33 mo, mean 30.8 mo) male Fischer Brown Norway (FBN) rats were used to collect data from 114 individual layer V neurons. Data from aged animals were compared with data from 105 young-adult male neurons (11 FBN rats, 4–6 mo) collected during the same time frame and using the same experimental protocol (Turner et al. 2005). Mean weights for young and aged FBNs were 356 and 525 g, respectively. All experiments were conducted in an International Acoustics Corporation sound-attenuating booth under a protocol approved by the Southern Illinois University School of Medicine Laboratory Animal Care and Use Committee. Experimentation was conducted in accordance with the Society for Neuroscience's Policy on the Use of Animals in Neuroscience Research and The American Physiological Society's Guiding Principles in the Care and Use of Animals.

Surgical protocol

Aged animals were initially anesthetized with a 1.1 ml/kg dose of a 3:1 mixture of ketamine:xylazine (100:20 mg/ml) and maintained for the remainder of the experiment (typically 10–12 h) on booster doses of urethane (ethyl carbamate, Sigma). Anesthesia level was monitored by observation of response to toe pinch and corneal reflex, and booster doses of urethane (500 mg/kg) were given as needed (about every 3 h). Aged animals were given about 80% of the dose given to young-adult animals to account for the altered metabolism with age (Boorman et al. 1990; Finlayson and Caspary 1993; Palombi and Caspary 1996). To verify that similar planes of anesthesia were achieved between young and aged animals, interdose intervals were measured and compared between age groups. Young animals required a booster dose every 194 min, whereas aged animals required a booster dose every 176 min. This difference in interdose intervals was not significant [$t(40) = 0.80$, $P = 0.42$], suggesting that young and aged animals were maintained under a similar plane of anesthesia using the prescribed dosing regimen. Urethane was selected after a series of pilot recordings from AI neurons in 10 FBN rats. Primary auditory cortex neurons recorded from urethane-anesthetized animals were more responsive to acoustic stimuli than cells under ketamine/xylazine or barbiturate (Turner, Hughes, and Caspary, unpublished observations). Urethane was also reported to have relatively minor affects on the GABAergic systems (Hara and Harris 2002; Maggi and Meli 1986).

Animals were placed on a homeothermic blanket with body temperature monitored by a rectal probe and maintained at 37°C. The dorsal surface of the skull was exposed, cleaned thoroughly and dried. A metal plate (1 cm^2) was attached to the dorsal skull with ethyl cyanoacrylate (Krazy Glue) and dental acrylic. After the glue and dental acrylic had dried completely, the metal plate was clamped to the stereotaxic apparatus to stabilize the head for the duration of the experiment. The skin was reflected from the lateral aspect of the skull, the temporalis muscle retracted, and a small craniotomy centered 5 mm caudal and 4 mm ventral to Bregma was performed to expose the left AI. A 3-mm-diameter ovoid craniotomy exposed a portion of AI as described by Games and Winer (1988), Paxinos and Watson (1998), Sally and Kelly (1988), and Zilles and Wree (1995). The dura was then carefully removed and the surface of AI kept moist with mineral oil. The center of the recording field was always 5 mm caudal and 4 mm ventral to Bregma. A single isolated unit was recorded from each of the six to ten electrode penetrations per animal. If one unit was isolated in superficial layer V, it was sometimes possible to advance the electrode and isolate a second unit in a deeper portion of layer V. The operational criteria for recording AI layer V neurons included correct stereotaxic coordinates, electrode depth of 600–950 μ from the pial surface (Games and Winer 1988) as measured by a Burleigh 6000 series microdrive (Fishers, NY) and the presence of a robust acoustically evoked "slow wave." The slow wave is a summed multiunit/synaptic response ≤50 ms in duration observed when no low-pass filter is applied. The slow wave is an estimate of a column's driven activity. The slow wave can be reliably tuned and used for assessing the tonotopic locus of the recording electrode.

Calibration, recording, and juxtacellular procedures

Acoustic signals were generated using Tucker Davis Technologies (TDT) System II hardware (Gainesville, FL), amplified (Phase 3, HA-2B) and transduced with an earphone (Beyerdynamic DT931, Farmingdale, NY) juxtaposed to the right ear canal (with pinna removed) using polypropylene tubing (7.7 cm in length). The sound system was calibrated using a ¼-in. Brüel & Kjær model 4136 microphone (Nærum, Denmark) and a simulated rat ear (Palombi and Caspary 1996). Calibration software performed a Fourier analysis on the signal-generation system in response to a 1Vrms click to generate calibration tables in dB sound pressure level [SPL re: 20 microPascals (μPa)] for use by programmable attenuators (software from Boston University, Drs. K. Hancock and H. Voigt). The resulting pure-tone intensities in dB SPL were accurate within 2 dB for frequencies between 0.5 and 50 kHz. Signal generation and data acquisition were controlled by Windows-based interactive Boston University software. Search stimuli consisted of broadband noise, pure tones, and frequency-modulated stimuli. All putative layer V single neurons were included in the present study. This included healthy neurons responding sluggishly or irregularly to acoustic stimuli, spontaneously active neurons inhibited by acoustic stimuli or neurons with no obvious responses to acoustic stimuli. In addition, resistance changes in the recording electrode sometimes suggested a neuronal membrane was present but the neuron was not firing in response to search stimuli. In cases where the putative neuron apparently did not respond to acoustic stimuli, small amounts of search current (1–10 nA, constant positive polarity) were passed through the electrode tip to confirm the presence of a nonresponsive neuron. When a cell responded to the current stimulation, a complete stimulus set would be obtained. If a cell did not respond to the current, the electrode would be advanced using current and sound until the presence of a cell could be verified. Current was used only when the tip resistance of the electrode suggested a nonresponsive neuron was near. Using current to verify the presence of quiet/sluggish neurons undoubtedly yielded a more inclusive neuron sample. However, such "quiet" neurons could yield important information for signal processing, particularly with respect to inhibitory mechanisms (Dykes et al. 1984; Foeller et al. 2001; Wang et al. 2000, 2002).

Glass recording electrodes were vertically pulled (Kopf 720) and beveled to a tip resistance of 10–20 MΩ. Electrodes were filled with 2 M KAc, 4% Sigma type VI HRP in 0.5 M KCl Tris buffer or 2.5% Neurobiotin (Vector) in 0.5 M KAc and advanced perpendicularly through AI layers using a Burleigh piezoelectric micropositioner. Signals were recorded by a silver-chlorided silver wire coupled to a head stage of a preamplifier (Dagan 8100). Spikes were discriminated using a window discriminator (Model 120, W-P Instruments, Sarasota, FL) and recorded using an event timer (TDT, ET-1) with a 1.0-μs resolution and saved to disk for later analysis. Responses to current stimulation and juxtacellular labeling used positive current pulses (1–10 nA) of 200-ms duration delivered through the balanced bridge of the preamplifier. Current was triggered and controlled through an S44 Grass Stimulator (West Warwick, RI). Responses to current pulse stimulation were collected as poststimulus time histograms (PSTHs) in response to 100 presentations of the current stimulus. Juxtacellular labeling followed the technique of Pinault (1996). The electrode was advanced until resistance changes and action potential amplitude suggested the somatic membrane was near. Current pulses were then presented at increasing amplitudes (≤10 nA) while carefully advancing the electrode in 1-μm steps until relatively low levels of the current (often as little as 1–3 nA) could drive the

neuron. At that point, both the collection of spikes in response to current stimulation as well as Neurobiotin electroporation was attempted.

Three successive repetitions of a pure-tone receptive field map (RM) were obtained from all layer V neurons. Each RM consisted of ≤720 pure-tone stimuli (50-ms duration, 5-ms rise/fall, 2-Hz presentation rate) at combinations of 40 frequencies (0.1-octave steps) and 18 intensities (0–85 dB SPL) with one stimulus per frequency/intensity point in the map. The rationale for using one trial per stimulus frequency/intensity combination was to track cortical variability by looking specifically at RM variability from one RM to the next by using correlational analysis. Data from the companion paper in young-adult neurons (Turner et al. 2005) suggested that focusing on variability using these methods in cortex might prove useful to understanding the plastic changes that occur with aging in AI. Traditional approaches often use several trials at each frequency/intensity combination, which effectively averages the response at each point in the RM and minimizing variability, thus preventing an examination of subtle age-related changes in variability across repetitions.

RM stimuli were sometimes centered on best frequency as determined from search tones, but in most cases were centered in the middle of the rat audible range (12–20 kHz) to obtain a relatively complete picture of the spectral receptive field of the neuron. RM stimuli were presented in a "fanning out" fashion beginning at the center frequency and stepping 0.1 octave to the high side (0–85 dB), followed by a 0.1-octave step to the low side of center, then back to the high side, and so forth. Receptive fields were plotted automatically by first calculating the spike rate from 0 to 70 ms (50-ms stimulus) and comparing that to the unit's baseline firing rate in the 430- to 500-ms poststimulus period. The 70-ms window was chosen based on known latencies of AI units as well as observations of typical responses of layer V neurons to acoustic stimuli. For a particular frequency/intensity point in the map, spike rates within the stimulus window exceeding 120% of the baseline firing rate were plotted as excitatory, whereas spike rates <80% of baseline were plotted as inhibitory. The receptive field map was then smoothed using a nine-point spatial filter, whereby the color code at each frequency/intensity point in the map represented the mean firing rate at that point and its eight nearest neighbors. In addition, spontaneous activity levels for each neuron were collected separately using 20-s trials with no acoustic stimulus. Responses to more complex stimuli such as narrowband noise, broadband noise, sinusoidal amplitude-modulated and frequency-modulated stimuli were collected, but are not presented here. In addition, PSTHs were collected for a subset of neurons in response to a 200-ms current pulse ranging from 1 to 10 nA. Current PSTHs were always collected at the end of the data collection protocol for each neuron. Current PSTHs were used to determine the current responsiveness of neurons independent of their responses to sound. Complete data collection protocol for each neuron lasted between 45 and 60 min depending on whether current responses were collected.

Histology

Electrode locations were confirmed by reconstructing tracts with the help of 4% HRP (Sigma) injections to mark the recording location, or in some cases, by filling individual cells with 2.5% Neurobiotin (Vector Laboratories) using juxtacellular electroporation recording techniques following the method of Pinault (1996). Each animal was perfused transcardially until clear with 0.9% normal saline, followed by 300 ml of 4% paraformaldehyde in 0.1 M phosphate buffer. To better preserve fine dendritic detail in Neurobiotin-injected tissue, 2% paraformaldehyde and 1.25% glutaraldehyde in 0.1 M phosphate buffer was used as a fixative. After perfusion, the brain was removed and stored in fixative overnight at 4°C. In experiments where HRP was injected to mark the electrode location, the brain was immersed in increasing concentrations of sucrose ≤20% and cryostat sectioned in the frontal plane at 40–60 μm. Sections were then processed for HRP using DAB (Sigma). In experiments using juxtacellular labeling with 2.5% Neurobiotin, vibratome sections were cut at 60–100 μm and visualized using either a streptavidin conjugated with fluorescein or HRP (Vector) then processed through DAB.

Data reduction and statistical analysis

The three repetitions of the RMs were first scored by three independent raters on their *1*) consistency (five-point Likert scale from no change to dramatic receptive-field change across the repetitions) and *2*) excitatory response-area shape. Excitatory response areas were initially classified using the nine categories in auditory cortex proposed by Sutter (2000). However, on further inspection, it was found that layer V RMs could be broken down into just five categories, dominated by receptive fields characterized as: *1*) the "classic" V/U-shaped tuning curve common in lower auditory structures; *2*) Complex receptive field maps characterized by "spotty" excitatory and inhibitory areas, which were inconsistent across the three repetitions; *3*) neurons that appeared to have shape and reliability characteristics intermediate between the V/U and Complex types; *4*) neurons with highly nonmonotonic hot spots, which were consistent across the three repetitions; and *5*) neurons with a high threshold.

Quantifying the three repetitions of the receptive field map involved calculating the spike rate (spikes/s) both inside the stimulus window (0–70 ms) and outside the stimulus window (71–500 ms) for each frequency/intensity stimulus point in the receptive field. Spike rates were converted to a single value that expressed the relative excitatory/inhibitory drive index at that point

$$\text{Drive index} = \frac{(\text{firing rate during stimulus} - \text{firing rate poststimulus})}{(\text{firing rate during stimulus} + \text{firing rate poststimulus})}$$

This index value was calculated for each frequency/intensity point in each of the three consecutive RMs and used to compute a Pearson correlation between runs 1 and 2, 1 and 3, and 2 and 3. A mean correlation across the three runs was then computed for each point in the receptive field and collapsed to form a single grand mean correlation index to represent the three runs of the receptive field maps for each neuron. In addition to Pearson correlations, standard ANOVA techniques were used for inferential statistical analyses.

RESULTS

Complete data were obtained from 114 neurons from aged animals determined to be from AI layer V and compared with a similar set of 105 units from young-adult rats (young data published in Turner et al. 2005). Mean recording depth for layer V neurons was 746 μm in aged rats and 760 μm in young-adult rats, roughly halfway between the layer V boundaries (600–950 μm) as defined by Games and Winer (1988). Young-adult rat AI typically measures 1.2 mm from pial surface to white matter. Aged rats often show 10–12% shrinkage to approximately 1.1 mm total AI thickness. In both age groups the mean recording depths placed the electrode tip in the approximate center of layer V, which extends from 50 to 75% of the total cortical thickness (Games and Winer 1988). All labeled neurons and HRP marks were verified histologically to be within the boundaries of AI layer V. Young-adult neurons driven by acoustic stimuli had a significantly shorter mean response latency (18.5 ms) than neurons from aged rats (23.1 ms) [$F(1,139) = 9.70$, $P = 0.002$]. Latency variability was also significantly greater for neurons from aged rats (variance = 115.0) compared with young (variance = 43.1) when using an F-test for variances [F(75 df young, 64 df aged), $P < 0.001$]. Mean best frequency (BF), defined as the fre-

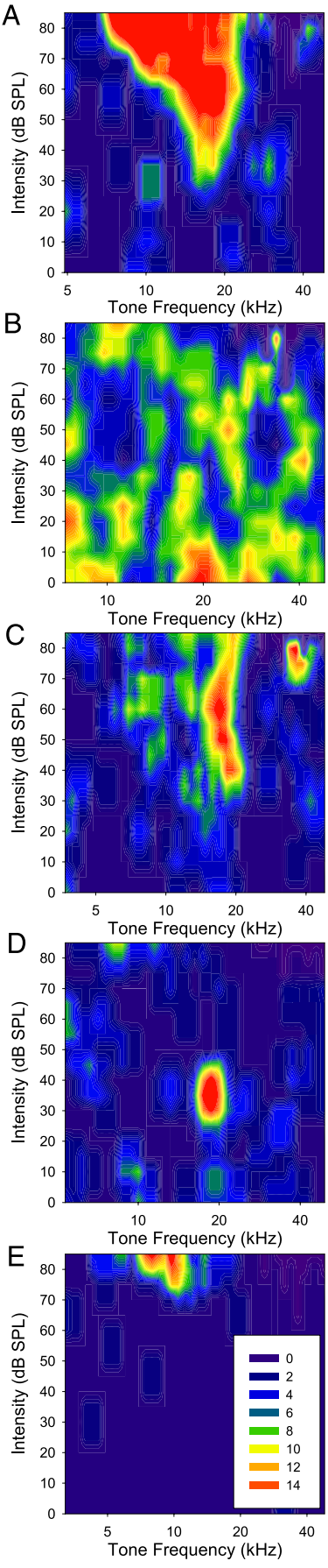

quency with the highest firing rate, and spread (SD) were nearly identical in neurons from young (23.6 kHz, 15.0 SD) and aged (23.5 kHz, 14.7 SD) rats, suggesting a consistent sampling across age from the middle tonotopic region of AI. Ranges of BFs were 2–50 kHz in young rats and 4–50 kHz in aged rats. Receptive fields for layer V neurons in aged rats exhibited flat threshold elevations of about 20 dB SPL, consistent with previous work in the FBN rat (Turner and Caspary 2005).

Two major receptive field types

Similar to young-adult animals (Turner et al. 2005), aged layer V RMs consisted of five major types, two of which comprised 75% of the total layer V data set (Fig. 1). Of 114 layer V neurons, 24 (21%) displayed strong responses to pure tones that resembled classic "V/U"-shaped excitatory RMs similar to those described for neurons in many lower auditory structures (Fig. 1*A*). Most showed low-side sloping "V"- or "U"-shaped excitability with responses virtually unchanged across three sequential RM repetitions. By contrast, 54% (61/114) of layer V neurons displayed Complex receptive fields characterized by inconsistent responding, occasional inhibition of spontaneous activity by acoustic stimuli, weak stimulus-driven excitation, and nonmonotonic firing (Fig. 1*B*). If discernable, the frequency with lowest threshold generally varied across sequential receptive field map repetitions, and regions within a given RM could change from excitation to inhibition on successive runs of the map. Three less common receptive field-response maps were also identified. Of 114 sample units, 19 (17%) displayed responses similar to V/U-shaped excitatory responses in Fig. 1*A*, but with high levels of variability across the three repetitions, and were thus placed into a third "Intermediate" category (Fig. 1*C*). Some of these units displayed V/U-shaped characteristics in at least one repetition of the RM. Of 114 layer V neurons, four (4%) displayed consistent, strongly nonmonotonic "hot spot" or closed tuning curve receptive fields (Fig. 1*D*). The remaining 5% (6/114) displayed high thresholds, which made their shape difficult to categorize (Fig. 1*E*).

Although the same basic types of RMs were present in neurons from young and aged rats, aging was also associated with a significant change in the distribution of receptive field shapes (Fig. 2). A smaller percentage of V/U-shaped receptive fields and a larger percentage of both Complex and Intermediate receptive fields were encountered in aged rats. This altered distribution was verified between young and old neurons using a chi-square test [$\chi^2(3) = 8.64$, $P = 0.03$].

FIG. 1. Major types of receptive fields in aged rat primary auditory cortex (AI) layer V. Aged rats, similar to young adults, exhibited 5 major types of receptive field maps (RMs) in AI layer V: V/U-shaped tuning curves similar in shape to those commonly found at lower levels of the auditory system (*A*); Complex RMs, so named because of the apparent complexity and unpredictability of their receptive fields (*B*); a category of RMs intermediate to *A* and *B* (*C*); highly nonmonotonic "hot spot" RMs (*D*); and RMs with high thresholds (*E*). *x*-axis represents pure-tone frequency (≤50 kHz); *y*-axis, pure-tone intensity; and *z*-axis, firing rate relative to spontaneous activity. Note color calibration chart in *E*, whereby "hotter" colors (i.e., yellows-reds) indicate higher stimulus-driven firing rates.

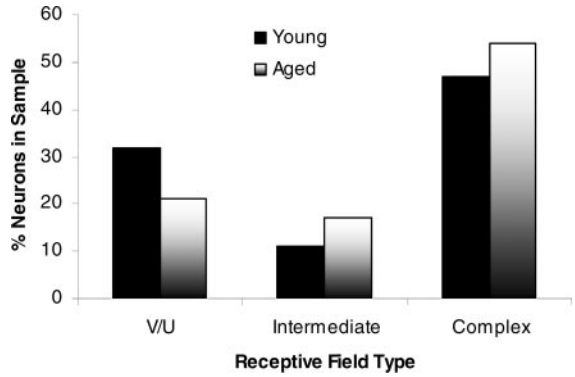

FIG. 2. Distribution of RM shapes in young and aged rats. Age was associated with fewer classic V/U-shaped RMs and more Intermediate and Complex types. Change in RM distribution between young and old animals was statistically significant (χ^2, $P < 0.05$).

Excitatory/inhibitory drive index

Neurons in aged rats also demonstrated significant differences in their responses to acoustic stimulation. In young animals, V/U-shaped neurons demonstrated clear excitatory drive in response to acoustic stimulation, whereas Complex neurons demonstrated a more inhibitory drive index. Divergent response properties displayed by the two major types of neurons in layer V (V/U excited and Complex inhibited by sound) appeared to be tempered somewhat with old age. Using mean excitatory/inhibitory drive index data from runs 1–3, neurons from aged rats overall trended (although not significantly) toward displaying more off-stimulus firing [$F(1,209) = 3.51$, $P = 0.06$]. When the drive index was used to compare the different receptive field types, old V/U-shaped units displayed a significant increase in off-stimulus firing when compared with young V/U-shaped units [$F(1,54) = 12.64$, $P = 0.00$] (Fig. 3). The young versus old comparison for Complex units yielded a trend, but no significant difference in excitatory/inhibitory drive index [$F(1,102) = 3.81$, $P = 0.054$]. Averaging all points in the entire receptive field yielded an overall mean drive index. ANOVAs were then used to determine whether the drive index became significantly more excitatory or inhibitory across the three repetitions. No significant changes in overall drive index across repetitions were found for either age group between runs 1 and 2 (Young: $P = 0.70$; Aged: $P = 0.75$), 2 and 3 (Young: $P = 0.98$; Aged: $P = 0.84$), or 1 and 3 (Young: $P = 0.98$; Aged: $P = 0.91$).

RM reliability

Repeating the same map three times highlighted differences in map reliability between the two age groups (Fig. 4). Decreased response map reliability with age, across all receptive field shapes, was first verified by blinded ratings of map variability (Mann–Whitney U test for ranked data, $z = -2.38$, $P = 0.017$). Second, the drive index values for each point in the RMs were used to compute runwise correlations. This mean correlation, using all of the frequency/intensity points in each RM, was used to quantitatively determine the reliability present in the three runs (run 1 vs. 2, run 2 vs. 3, and run 1 vs. 3). This method also demonstrated a clear age-related decrease in reliability in the receptive field maps [$F(1,207) = 20.0$, $P = 0.00$] (Fig. 5). The decrease in map reliability with age appeared to be independent of receptive field shape. When comparing young versus old receptive field variability, significantly less reliability was observed for old V/U [$F(1,55) = 4.73$, $P = 0.03$] and Intermediate receptive fields [$F(1,29) = 5.99$, $P = 0.02$], whereas the differences for Complex receptive fields did not quite reach the 0.05 level of statistical significance [$F(1,102) = 3.45$, $P = 0.06$]. To determine whether age-related threshold changes explain the reduced reliability of aged RMs, correlations were also measured across repetitions in the spectral center of each unit's receptive field at a level of 80 dB SPL—a level ≥20 dB above threshold for aged FBN rats. The reduced reliability of RMs appears to be present in aged animals even for suprathreshold stimuli because a high correlation across repetitions was found in neurons from young rats, but not in aged. The correlation at 80 dB SPL from the first to third repetition was significantly higher in young rats ($r = +0.42$) compared with aged rats ($r = +0.11$) ($z = 2.51$, $P = 0.006$).

Current responses

Responses to current pulse stimulation delivered to the soma were also collected for a subset of 36 neurons. Young-adult V/U-shaped neurons were readily driven by current-pulse stimulation, whereas neurons showing Complex response maps were not easily driven by current (Turner et al. 2005). Although there did not appear to be significant age-related changes in the response to current-pulse stimulation of 11 young rat and five aged rat neurons with V/U-shaped RMs [$F(1,14) = 0.77$, $P = 0.39$], significant age-related changes were seen for neurons displaying Complex RMs. Complex RM neurons from young rats ($n = 7$) fired poorly in response to current, whereas Complex RM neurons from aged animals ($n = 13$) responded vigorously to current stimulation [$F(1,19) = 4.87$, $P = 0.04$]. This age-related change can be seen in the collapsed composite PSTH in Fig. 6 and individual PSTHs in Fig. 7.

Spontaneous activity

Single-unit spontaneous activity levels were not significantly different between young (spikes/s ± SE: 6.72 ± 0.68)

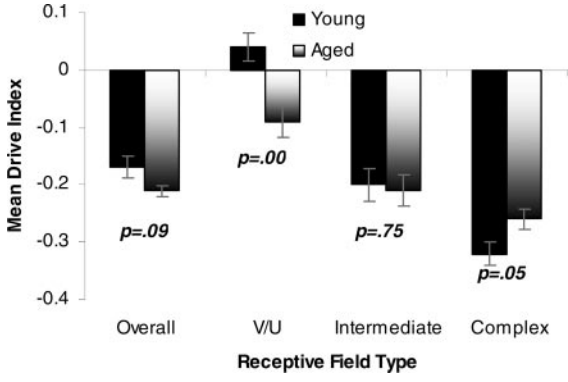

FIG. 3. Excitatory/inhibitory drive index as a function of RM shape. In normal, young-adult rats, V/U-shaped neurons were associated with more on-stimulus firing (higher drive index), whereas Complex RMs were associated with inhibition during the stimulus (lower drive index). This polarity of responses between the 2 RM types was somewhat reversed in aging.

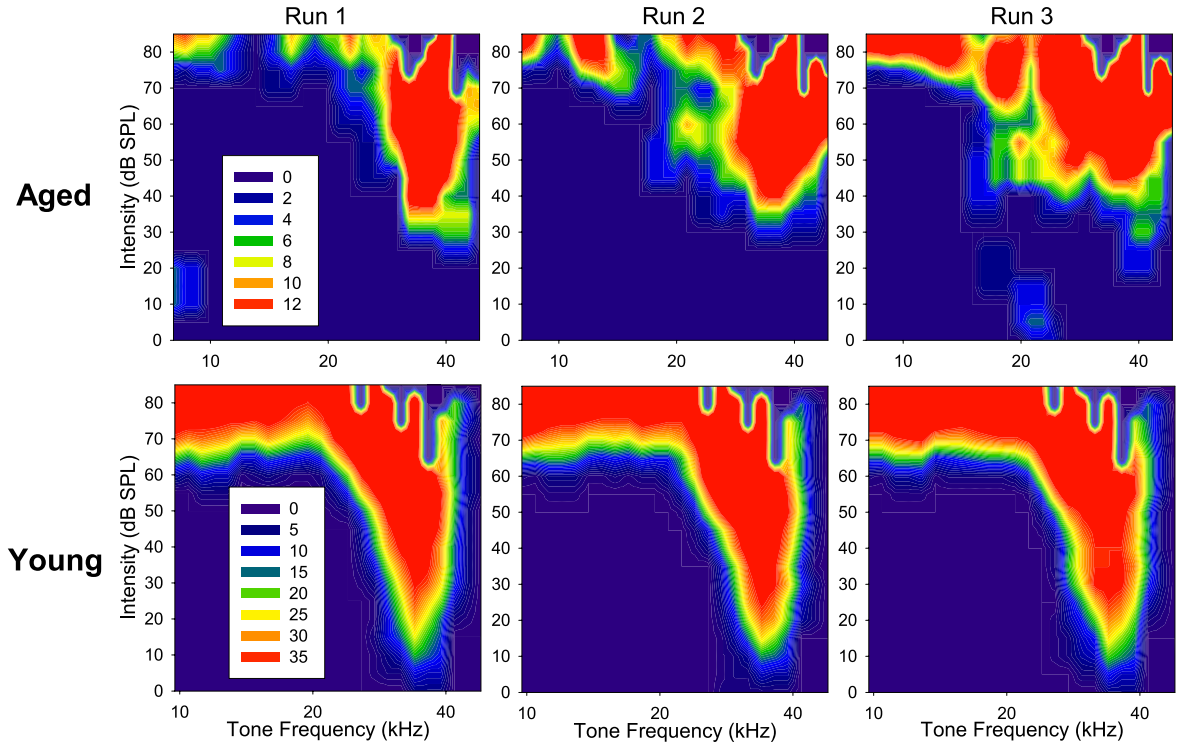

FIG. 4. Three successive repetitions of an RM for neurons from young and aged rats. These maps represent some of the best V/U-shaped maps in both the young and aged animals. In old RMs, the tip of the V reflects a 20-dB hearing loss. In addition to the clear differences at the peak of the tuning curves, repeating the same map 3 times demonstrated clear differences in variability between the 2 age groups (see Fig. 5). Young plot adapted from Turner et al. (2005).

and aged rats overall (6.36 ± 0.62) [$F(1,219) = 0.15$, $P = 0.70$]. When spontaneous activity was compared across RM type (V/U vs. Complex) and Age (young vs. old) using a two-way ANOVA, neither RM type nor Age revealed a significant main effect [$F(1,164) = 1.06$, $P = 0.30$ and $F(1,164) = 0.19$, $P = 0.66$, respectively]. The Age × RM type interaction was also not significant [$F(1,164) = 1.38$, $P = 0.24$]. However, plotting the data suggests interesting trends whereby aging might be associated with subtle reductions in spontaneous activity in V/U-shaped neurons and increased spontaneous activity in Complex neurons (Fig. 8). Spontaneous activity rates were virtually identical between V/U and Complex types in young animals [$F(1,81) = 0.01$, $P = 0.91$]. However, in aged animals there was a nonsignificant trend for

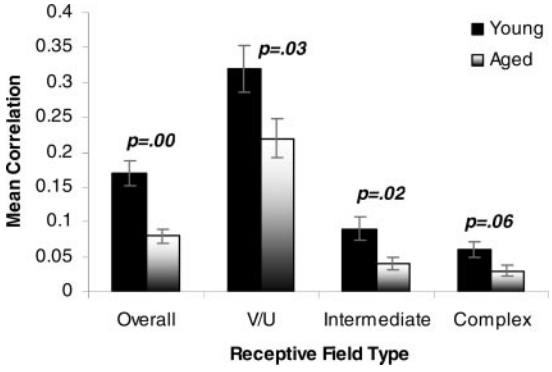

FIG. 5. Variability across RM repetitions. Neurons from aged animals demonstrated greater variability across the 3 consecutive runs of the RM. Increased variability with age appeared to occur independently of RM type.

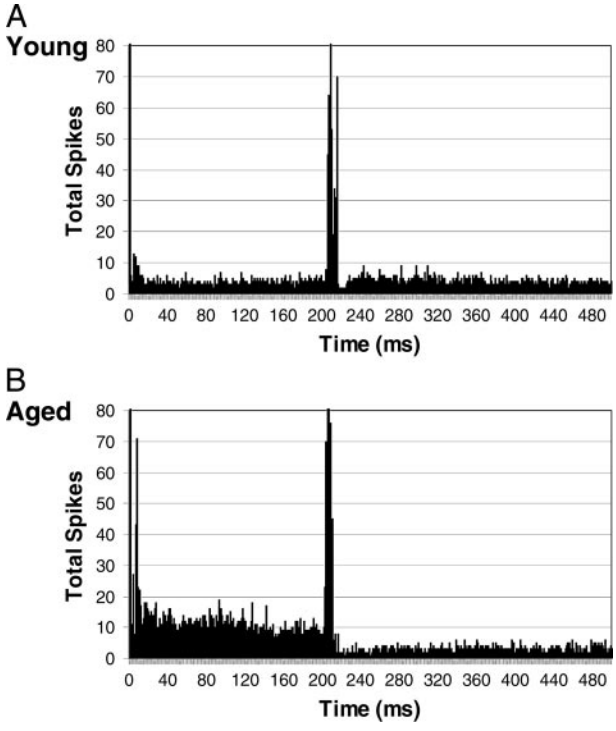

FIG. 6. Composite responses to current pulse stimulation combined for Complex RM neurons from young (*A*) and aged rats (*B*). Neurons with Complex RMs were difficult to drive by current pulses in young rats (*A*) compared with aged rats (*B*). Plots depict all Complex RMs collapsed across the 2 age groups for which current responses were collected ($n = 13$ aged, $n = 7$ young). No differences in responses to current stimulation were found in V/U-shaped RM neurons.

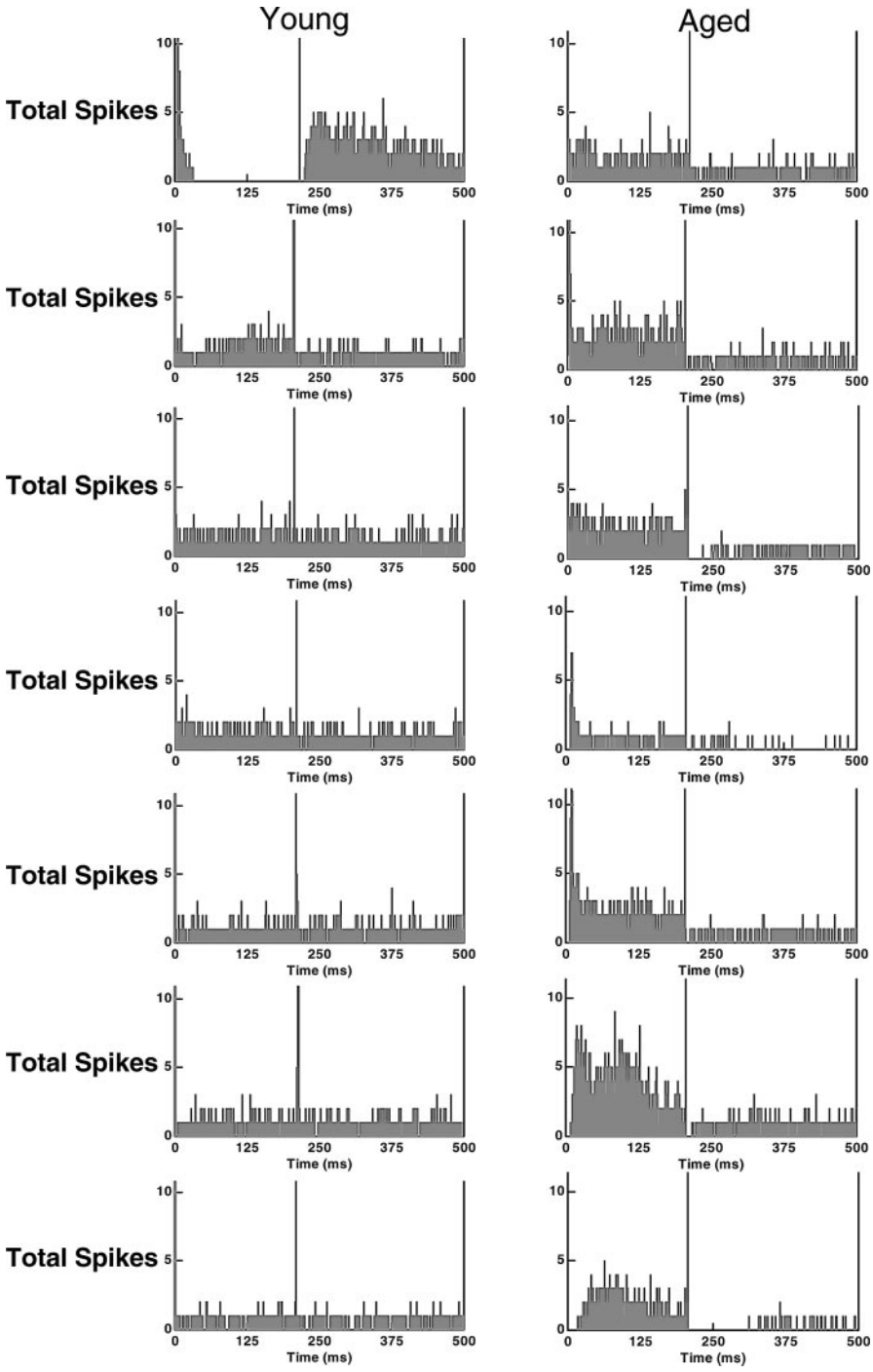

FIG. 7. Representative examples of poststimulus time histogram responses to current in young and aged Complex RM neurons. Neurons from young-adult rats (*A*) were difficult to depolarize with current pulses to the cell body, whereas the neurons from aged rats responded well to the same current pulses (*B*).

reduced spontaneous activity in V/U and increased spontaneous activity in Complex types [$F(1,83) = 2.39$, $P = 0.12$]. High levels of variability within groups made it difficult to demonstrate differences in spontaneous activity.

Finally, the two major types of RMs appeared intermingled within layer V of AI because there were no statistically reliable differences between the two types of RMs on depth of recording [V/U 767 μm vs. Complex 739 μm; $F(1,80) = 1.14$, $P = 0.289$]. In addition, the two types were frequently recorded in the same electrode tract in close anatomical and temporal proximity to one another.

DISCUSSION

Aged receptive field maps (RMs) in AI layer V neurons generally fell into one of two major categories. Like young-adult neurons, one type displayed classic tuning curves with V/U-shaped excitability, whereas the other type displayed highly variable receptive fields, which were previously termed Complex (Turner et al. 2005). However, aging was associated with several significant changes that could have implications for understanding the role the cortex plays in the symptoms of presbycusis. First, the distribution of receptive field shapes was

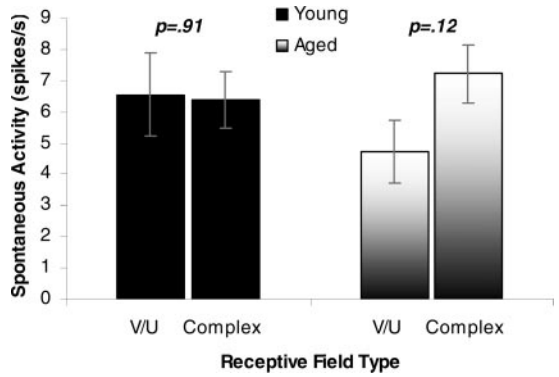

FIG. 8. Single-unit spontaneous activity levels (spikes/s) as a function of age and receptive field type. Spontaneous activity levels in V/U and complex RMs were no different in young and aged rats. However, a trend for reduced spontaneous activity in aged V/U RMs was evident.

altered in aging; V/U-shaped RMs were less common, whereas Complex and Intermediate RMs were more common. Second, aging differentially affected the stimulus-driven activity with neurons from aged rats exhibiting V/U-shaped RMs showing less on-stimulus firing, whereas more on-stimulus firing was seen for Complex RMs (which were generally associated with inhibited firing in young-adult controls). Third, RMs from aged rats, regardless of shape, were less reliable across three successive RM repetitions for each neuron. Fourth, aging in Complex RMs, but not V/U RMs, was associated with a hyperexcitable response to extracellular current pulse stimulation. Finally, neurons with Complex RMs trended toward an age-related increase in spontaneous activity relative to aged V/U-shaped RMs.

The two major divergent receptive field shapes are thought to convey different stimulus information (Turner et al. 2005) and likely have different projection patterns (Hefti and Smith 2000, 2003). V/U-shaped RM neurons were more closely associated with larger pyramidal cells that form the descending projections to the brain stem (Games and Winer 1988; Turner et al. 2005; Winer and Prieto 2001; Winer et al. 1998). In contrast, neurons with the Complex RMs were associated with smaller layer V cells that are thought to exhibit a more local projection pattern and greater inhibitory tone (Hefti and Smith 2000, 2003; Turner et al. 2005). Although the underlying causes for the age-related changes in AI have not been fully elucidated, recent findings suggest that γ-aminobutyric acid (GABA) circuits shape response properties of auditory cortex neurons (Foeller et al. 2001; Wang et al. 2000, 2002) and that significant pre- and postsynaptic age-related changes occur in these GABA systems. Aging in AI has been associated with reduced GABA content across all layers, reduced receptor binding of radioactive $GABA_A$ agonists, as well as remodeling of the postsynaptic $GABA_A$ receptor (Caspary et al. 2003; Ling et al. 2005). Pre- and postsynaptic changes to the GABA system could have major impacts on the response properties of AI neurons. It is not known whether changes to the AI GABA system are confined to certain types of presynaptic GABAergic cells or to certain types of postsynaptic targets in AI (e.g., $GABA_A$ receptors on the soma vs. on the dendritic branches). Hefti and Smith (2000, 2003) found that smaller pyramidal neurons (presumably those showing Complex RM responses in the present study) were more sensitive to $GABA_A$ receptor blockade. This suggests greater somatic input onto these neurons relative to the large pyramidal neurons associated with V/U RMs. Data from the present study suggest that aging might have a relatively greater impact on the GABA contacts of Complex RM neurons. If aging is associated with a downregulation of inhibitory tone, it might be expected that Complex RMs, which show strong inhibitory control over neural firing, would be differentially impacted by aging. Future studies that incorporate characterization of receptive field shape, intracellular and/or juxtacellular labeling of the cell, and immunocytochemical identification of the distribution of GABA contacts on the cell are necessary to directly resolve this question. If aging is shown to have a preferential impact on one type of AI cell over the other, then appropriate pharmacological, environmental, or genetic therapeutics could be targeted to correct that specific circuit.

The relative reduction of V/U-shaped RMs and increase in Complex and Intermediate types of RMs could have significant implications for auditory processing in aged animals. The loss of the tips of the tuning curves with presbycusis, in combination with a reduction of finely tuned V/U-shaped receptive fields and reduced discharge rate, would affect descending pathways. Similarly, the relative increase in the more poorly tuned Complex and Intermediate types of receptive fields, as well as their reduced inhibitory response to sound, might serve to introduce more noise into AI and cortical coding of sound in general. Together, RM changes observed in the two major types of aged auditory cortex neurons could translate into degraded coding of acoustic signals, especially in complex acoustic environments.

In the present study, receptive fields in aged neurons were significantly less reliable when presented the same set of acoustic stimuli over three successive repetitions. The reduced reliability across runs was also found for an 80-dB SPL stimulus in the spectral center of each RM. This finding suggests that the mild, 20-dB threshold elevations present in the FBN rat model (Turner and Caspary 2005) cannot explain the reduced reliability in the aged receptive fields. Reduced reliability of driven activity could serve to reduce the accuracy of signal processing and increase noise within the temporal processor, potentially reducing the quality of the percept. A number of age-related changes could contribute to the increased variability observed in RMs from aged layer V neurons. Loss of peripheral cochlear function resulting in diminished input to the auditory neuroaxis could be followed by a selective loss of inhibition at the level of the brain stem, resulting in a loss of temporal resolving power and increased variability (Backoff and Caspary 1994; Barsz et al. 2002; Boettcher et al. 1996; Poth et al. 2001; Walton et al. 1998). This could then be conveyed to the level of the auditory cortex. De novo age-related changes at the level of neocortex could also explain the increased variability. Possible age-related changes at the level of the cortex include: a diminished role of intracortical GABA in shaping response properties, purely anatomical age-related changes including global damage to myelin sheaths in aging (Peters 2002), changes in AI layer V neuroglial cells (Vaughan and Peters 1974), deterioration of layer V pyramidal cell basal dendrites (Vaughan 1977), or reduction in layer V pyramidal cell body diameter and nuclear area. Although further studies will be needed to define the

location and the nature of changes, the present findings suggest that aging is associated with functional changes in AI layer V, which could account, in part, for the role the cortex plays in the speech understanding and other processing deficits seen in presbycusis (Tremblay et al. 2002, 2003). Whether the present findings are the consequence of changes in layer V of AI or whether these functional deficits are inherited from earlier centers of the auditory system is not clear. Current studies are under way comparing responses across cortical layers to determine whether similar deficits are found, for example, at input layers (III/IV) of AI.

Future studies parsing age-related changes in specific AI circuits should help in developing a more complete picture of the central components of presbycusis. In this context, a number of questions relating aging and hearing become germane. Are observed changes the result of hearing loss or are they relatively independent effects of aging? What role does auditory experience and training (as in hearing aids) play in differentially affecting specific AI circuits? In the present study and related neurochemical studies (Caspary et al. 2003; Leventhal et al. 2003), can age-related deficiencies in GABA neurotransmission in sensory neocortex be explained by altered functioning of just one of these types of neurons? Future studies should help clarify the role of these two types of layer V neurons in the central auditory system and can provide valuable information about their more global role in cortical information processing. Better understanding of the neurochemical and functional deficits in AI could lead to selective pharmacotherapy aimed at alleviating symptoms of presbycusis by replacing lost inhibitory function.

ACKNOWLEDGMENTS

Thanks to L. Ling and J. Parrish for helpful comments on the manuscript. Also thanks to Dr. Kenneth Hancock for work designing the stimulus control, data-acquisition, and calibration programs used in this study.

GRANTS

This work was supported by National Institutes of Health Grants AG-023910-01 to J. G. Turner and DC-00151 to D. M. Caspary and an Excellence in Academic Medicine grant to L. F. Hughes.

REFERENCES

Aitkin LM, Kenyon CE, and Philpott P. The representation of the auditory and somatosensory systems in the external nucleus of the cat inferior colliculus. *J Comp Neurol* 196: 25–40, 1981.

Backoff PM and Caspary DM. Age-related changes in auditory brainstem responses in Fischer-344 rats: effects of rate and intensity. *Hearing Res* 73: 163–172, 1994.

Barsz K, Ison JR, Snell KB, and Walton JP. Behavioral and neural measures of auditory temporal acuity in aging humans and mice. *Neurobiol Aging* 23: 565–578, 2002.

Bergman M, Blumenfeld VG, Cascardo D, Dash B, Levitt H, and Margulies MK. Age-related decrement in hearing for speech. Sampling and longitudinal studies. *J Gerontol* 31: 533–538, 1976.

Boettcher FA, Mills JH, Swerdloff JL, and Holley BL. Auditory evoked potentials in aged gerbils: responses elicited by noises separated by a silent gap. *Hearing Res* 102: 167–178, 1996.

Boorman GA, Eustis SL, Elwell MR, Montgomery CA Jr, and MacKenzie WF. *Pathology of the Fischer Rat: References and Atlas*. San Diego, CA: Academic Press, 1990.

Caspary DM, Ling L, and Hughes LF. Layer-specific age-related changes of GAD in rat primary auditory cortex. *Assoc Res Otolaryngol Abstr* 720, 2003.

Corso JF. Sensory processes and perception in aging. In: *Lectures on Gerontology*, edited by Viidik A. London: Academic Press, 1982, p. 441–479.

Divenyi PL and Haupt KM. Audiological correlates of speech understanding deficits in elderly listeners with mild-to-moderate hearing loss. I. Age and lateral asymmetry effects. *Ear Hear* 18: 42–61, 1997a.

Divenyi PL and Haupt KM. Audiological correlates of speech understanding deficits in elderly listeners with mild-to-moderate hearing loss. II. Correlation analysis. *Ear Hear* 18: 100–113, 1997b.

Doucet JR, Rose L, and Ryugo DK. The cellular origin of corticofugal projections to the superior olivary complex in the rat. *Brain Res* 925: 28–41, 2002.

Dykes RW, Landry P, Metherate R, and Hicks TP. Functional role of GABA in cat primary somatosensory cortex: shaping receptive fields of cortical neurons. *J Neurophysiol* 52: 1066–1093, 1984.

Finlayson PG and Caspary DM. Response properties in young and old Fischer-344 rat lateral superior olive neurons: a quantitative approach. *Neurobiol Aging* 14: 127–139, 1993.

Foeller E, Vater M, and Kossl M. Laminar analysis of inhibition in the gerbil primary auditory cortex. *J Assoc Res Otolarngol* 2: 279–296, 2001.

Games KD and Winer JA. Layer V in rat auditory cortex: projections to the inferior colliculus and contralateral cortex. *Hearing Res* 34: 1–25, 1988.

Hara K and Harris RA. The anesthetic mechanism of urethane: the effects on neurotransmitter-gated ion channels. *Anesth Analg* 94: 313–318, 2002.

Hefti BJ and Smith PH. Anatomy, physiology, and synaptic responses of rat layer V auditory cortical cells and effects of intracellular GABA(A) blockade. *J Neurophysiol* 83: 2626–2638, 2000.

Hefti BJ and Smith PH. Distribution and kinetic properties of GABAergic inputs to layer V pyramidal cells in rat auditory cortex. *J Assoc Res Otolaryngol* 4: 106–121, 2003.

Herbert H, Aschoff A, and Ostwald J. Topography of projections from the auditory cortex to the inferior colliculus in the rat. *J Comp Neurol* 304: 103–122, 1991.

Lee HJ, Wallani T, and Mendelson JR. Temporal processing speed in the inferior colliculus of young and aged rats. *Hearing Res* 174: 64–74, 2002.

Leventhal AG, Wang Y, Pu M, Zhou Y, and Ma Y. GABA and its agonists improved cortical function in senescent monkeys. *Science* 300: 812–815, 2003.

Ling LL, Hughes LF, and Caspary DM. Age-related loss of the GABA synthetic enzyme glutamic acid decarboxylase in rat primary auditory cortex. *Neuroscience* 132: 1103–1113, 2005.

Maggi CA and Meli A. Suitability of urethane anesthesia for physiopharmacological investigations in various systems. Part 1: General considerations. *Experientia* 42: 109–114, 1986.

Mendelson JR and Lui B. The effects of aging in the medial geniculate nucleus: a comparison with the inferior colliculus and auditory cortex. *Hearing Res* 191: 21–33, 2004.

Mendelson JR and Ricketts C. Age-related temporal processing speed deterioration in auditory cortex. *Hearing Res* 158: 84–94, 2001.

Ostroff JM, McDonald KL, Schneider BA, and Alain C. Aging and the processing of sound duration in human auditory cortex. *Hearing Res* 181: 1–7, 2003.

Palombi PS and Caspary DM. GABA inputs control discharge rate primarily within frequency receptive fields of inferior colliculus neurons. *J Neurophysiol* 75: 2111–2219, 1996.

Paxinos G and Watson C. *The Rat Brain in Stereotaxic Coordinates* (4th ed.). San Diego, CA: Academic Press, 1998.

Peters A. The effects of normal aging on myelin and nerve fibers: a review. *J Neurocytol* 31: 581–593, 2002.

Pinault D. A novel single-cell staining procedure performed in vivo under electrophysiological control: morpho-functional features of juxtacellularly labeled thalamic cells and other central neurons with biocytin or neurobiotin. *J Neurosci Methods* 65: 113–136, 1996.

Poth EA, Boettcher FA, Mills JH, and Dubno JR. Auditory brainstem responses in younger and older adults for broadband noises separated by a silent gap. *Hearing Res* 161: 10–18, 2001.

Sally SL and Kelly JB. Organization of auditory cortex in the albino rat: sound frequency. *J Neurophysiol* 59: 1627–1638, 1988.

Schofield BR and Coomes DL. Auditory cortical projections to the cochlear nucleus in guinea pigs. *Hearing Res* 199: 89–102, 2005.

Seidman MD, Ahmad N, and Bai U. Molecular mechanisms of age-related hearing loss. *Ageing Res Rev* 1: 331–343, 2002.

Sutter ML. Shapes and level tolerances of frequency tuning curves in primary auditory cortex: quantitative measures and population codes. *J Neurophysiol* 84: 1012–1025, 2000.

Tremblay KL, Piskosz M, and Souza P. Aging alters the neural representation of speech cues. *Neuroreport* 13: 1865–1870, 2002.

Tremblay KL, Piskosz M, and Souza P. Effects of age and age-related hearing loss on the neural representation of speech cues. *Clin Neurophysiol* 114: 1332–1343, 2003.

Turner JG and Caspary DM. Comparison of two rat models of aging: peripheral pathology and GABA changes in the inferior colliculus. In: *Plasticity and Signal Representation in the Auditory System*, edited by Syka J and Merzenich MM. New York: Springer-Verlag, 2005, p. 217–225.

Turner JG, Hughes LF, and Caspary DM. Divergent response properties of layer V neurons in rat primary auditory cortex. *Hearing Res* 202: 129–140, 2005.

Vaughan DW. Age-related deterioration of pyramidal cell basal dendrites in rat auditory cortex. *J Comp Neurol* 171: 501–515, 1977.

Vaughan DW and Peters A. Neuroglial cells in the cerebral cortex of rats from young adulthood to old age: an electron microscope study. *J Neurocytol* 3: 405–429, 1974.

Vaughan DW and Vincent JM. Ultrastructure of neurons in the auditory cortex of ageing rats: a morphometric study. *J Neurocytol* 8: 215–228, 1979.

Walton JP, Frisina RD, and O'Neill WE. Age-related alteration in processing of temporal sound features in the auditory midbrain of the CBA mouse. *J Neurosci* 18: 2764–2776, 1998.

Wang J, Caspary D, and Salvi RJ. GABA-A antagonist causes dramatic expansion of tuning in primary auditory cortex. *Neuroreport* 11: 1137–1140, 2000.

Wang J, McFadden SL, Caspary D, and Salvi R. Gamma-aminobutyric acid circuits shape response properties of auditory cortex neurons. *Brain Res Interact* 944: 219–231, 2002.

Willott JF. *Aging and the Auditory System: Anatomy, Physiology, and Psychophysics*. San Diego, CA: Singular Publishing, 1991.

Willott JF. Physiological plasticity in the auditory system and its possible relevance to hearing aid use, deprivation effects, and acclimatization. *Ear Hear* 17, *Suppl*. 3: 66S–77S, 1996a.

Willott JF. Anatomic and physiologic aging: a behavioral neuroscience perspective. *J Am Acad Audiol* 7: 141–151, 1996b.

Willott JF, Aitkin LM, and McFadden SL. Plasticity of auditory cortex associated with sensorineural hearing loss in adult C57BL/6J mice. *J Comp Neurol* 329: 402–411, 1993.

Winer JA, Larue DT, Diehl JJ, and Hefti BJ. Auditory cortical projections to the cat inferior colliculus. *J Comp Neurol* 400: 147–174, 1998.

Winer JA and Prieto JJ. Layer V in cat primary auditory cortex (AI): cellular architecture and identification of projection neurons. *J Comp Neurol* 434: 379–412, 2001.

Zilles K and Wree A. Cortex: areal and laminar structure. In: *The Rat Nervous System* (2nd ed.), edited by Paxinos G. San Diego, CA: Academic Press, 1995, p. 649–685.